

A simple and versatile cold-atom simulator of Non-Abelian gauge potentials

Daniel Braun^{1,2}

¹Université de Toulouse, UPS, Laboratoire de Physique Théorique (IRSAMC), F-31062 Toulouse, France and
²CNRS, LPT (IRSAMC), F-31062 Toulouse, France

We show how a single, harmonically trapped atom in a tailored magnetic field can be used for simulating the effects of a broad class of non-abelian gauge potentials. We demonstrate how to implement Rashba or Linear-Dresselhaus couplings, or observe *Zitterbewegung* of a Dirac particle.

Simulating complex quantum systems with the help of trapped cold atoms has become a flourishing branch of quantum optics. The exquisite control and complex internal structure of cold atoms have allowed successful experimental simulation of systems and effects ranging from quantum phase transitions in the Bose-Hubbard model [1], over Anderson localization [2, 3], to cosmological models [4]. Recently, a lot of research efforts have been directed towards realization of Abelian or Non-Abelian gauge fields. By bathing an optical lattice in additional weak, non-resonant light that can create Raman-transitions between hyperfine levels, one can create artificial magnetic fields which can be extremely strong. Vortex formation in a BEC has been observed due to such artificial magnetic fields [5]. Even the creation of magnetic monopoles has been proposed [6]. Non-abelian gauge fields can be useful for studying spin-tronics materials with various spin-orbit couplings, Berry phases, or topologically protected qubits.

Most of these quantum simulations have been proposed or performed for atoms trapped in an optical lattice or Bose-Einstein condensates, requiring rather sophisticated experimental setups. Many physical systems are, however, interesting as single-particle systems. Such is the case e.g. for Anderson localization, the low-energy behavior of electrons in Graphene, or the relativistic motion of electrons that leads to the effect of *Zitterbewegung* [7]. It would be highly desirable to have a simple, versatile system that allows to simulate such single particle dynamics. We show here that such a system can be constructed from a single, harmonically trapped atom exposed to a suitably tailored real (physical) magnetic field. We show that by simply changing some gradients of different field components different non-Abelian gauge fields can be simulated, giving rise, for example, to Rashba or linear Dresselhaus coupling. We also show that *Zitterbewegung* should be easily observable. Abelian gauge fields can also be obtained, but are less interesting in the proposed setup, as they do not depend on position.

Consider a single atom of mass m trapped in a harmonic potential (frequency ω) and exposed to a magnetic field $\mathbf{B}(\mathbf{x}, t)$. For concreteness, let us assume a neutral atom in an optical dipole trap. The magnetic field should not be used for any part of the trapping, but be controllable independently of the trapping. We will also assume that the atom is cooled close to the ground state such

that approximating the trap by a harmonic potential in all three directions is indeed reasonable. The hamiltonian of the system reads

$$H = \frac{\mathbf{p}^2}{2m} + \frac{1}{2}m\omega^2\mathbf{x}^2 + g_J\mu_B\mathbf{B}(\mathbf{x}, t) \cdot \mathbf{J}/\hbar, \quad (1)$$

where g_J , μ_B , and \mathbf{J} are the g-factor, Bohr-magneton, and total angular momentum of the atom, and we have neglected the nuclear spin contribution in the Zeeman term. Suppose that the magnetic field varies slowly on the scale of the trapping potential, such that we can expand it in a power series about the origin $\mathbf{x} = 0$,

$$\mathbf{B}(\mathbf{x}, t) = \mathbf{B}(\mathbf{0}, t) + \sum_{i=1}^3 \nabla B_i \cdot \mathbf{x} \hat{e}_i + \mathcal{O}(\mathbf{x}^2), \quad (2)$$

with unit vectors \hat{e}_i in directions $i = 1, 2, 3 \equiv x, y, z$. We have neglected higher order terms starting with the second order. One can still include the second order, with consequences to be discussed below, but for the moment suppose that the magnetic field varies slowly enough over the length-scale of the atomic motion in the trap that the quadratic term in \mathbf{x} from expanding \mathbf{B} can indeed be neglected compared to the quadratic term describing the trapping potential.

The linear term in \mathbf{x} then leads to a coupling $\mathbf{x} \cdot \nabla(\mathbf{B} \cdot \mathbf{J}) \equiv \mathbf{x} \cdot \sum_i (\nabla B_i|_{\mathbf{x}=\mathbf{0}}) J_i$. Now let us canonically transform $\mathbf{x}/x_0 \rightarrow -\mathbf{p}/p_0$, $\mathbf{p}/p_0 \rightarrow \mathbf{x}/x_0$, where I have introduced the natural scales x_0 and p_0 of the canonical coordinates and momenta of the atom in the trap, $x_0 = \sqrt{\hbar/(m\omega)}$ and $p_0 = \sqrt{\hbar m\omega}$. The harmonic oscillator part in the hamiltonian is invariant under this transformation, but the \mathbf{x} in the Zeeman term becomes a $-\mathbf{p}$, and we get the transformed hamiltonian \tilde{H} ,

$$\tilde{H} = \frac{\mathbf{p}^2}{2m} + \frac{1}{2}m\omega^2\mathbf{x}^2 - \frac{e}{m}\mathbf{p} \cdot \mathbf{A} + g_J\mu_B\mathbf{B}(\mathbf{0}, t) \cdot \mathbf{J}/\hbar, \quad (3)$$

with

$$\mathbf{A} = \frac{\mu_B g_J}{e\hbar\omega} \nabla(\mathbf{B} \cdot \mathbf{J})_{\mathbf{x}=\mathbf{0}}. \quad (4)$$

Note that \mathbf{A} is independent of position and thus commutes with \mathbf{p} . We can therefore rewrite the hamiltonian in the form

$$\tilde{H} = \frac{1}{2m}(\mathbf{p} - e\mathbf{A})^2 + \frac{1}{2}m\omega^2\mathbf{x}^2 + \phi + \mu_B g_J \mathbf{B}(\mathbf{0}, t) \cdot \mathbf{J}/\hbar, \quad (5)$$

which makes appear \mathbf{A} as a gauge potential. The constant ϕ acts only in the angular-momentum Hilbert space,

$$\phi \equiv -\frac{e^2 \mathbf{A}^2}{2m}, \quad (6)$$

and can be considered an anisotropy for the angular momentum. We can write it as

$$\phi = -\frac{1}{2} \mathbf{J}^t I^{-1} \mathbf{J}, \quad (7)$$

where the inverse tensor of inertia I^{-1} has matrix elements

$$(I^{-1})_{ij} = \frac{\mu_B^2 g_J^2}{m \hbar^2 \omega^2} \nabla B_i \cdot \nabla B_j. \quad (8)$$

The effect created by the gauge potential plays an appreciable role only if the components of $e\mathbf{A}$ are comparable to the corresponding components of \mathbf{p} . The latter are, close to the ground-state of the harmonic potential, of the order of p_0 . With $\mathbf{J} \sim \hbar$, we are thus led to a condition for the magnitude of the magnetic field gradient B'

$$B' \sim \frac{\sqrt{\hbar m \omega}^{3/2}}{\mu_B}, \quad (9)$$

which should be satisfied for at least one component of \mathbf{B} . Inserting the data for ^{87}Rb , we find a gradient $B' = 2.1 \text{ Gauss/mm}$ for $\omega = 2\pi \cdot 1 \text{ kHz}$, which appears to be a very convenient order of magnitude.

It is worthwhile spelling out the components of \mathbf{A} explicitly. Up to the common prefactor $\frac{\mu_B g_J}{c \hbar \omega}$ we have

$$\mathbf{A}_x \propto \partial_x B_x J_x + \partial_x B_y J_y + \partial_x B_z J_z \quad (10)$$

$$\mathbf{A}_y \propto \partial_y B_x J_x + \partial_y B_y J_y + \partial_y B_z J_z \quad (11)$$

$$\mathbf{A}_z \propto \partial_z B_x J_x + \partial_z B_y J_y + \partial_z B_z J_z. \quad (12)$$

The components of \mathbf{J} are real physical angular momentum, and thus satisfy $[J_x, J_y] = i\hbar J_z$ in any Hilbert space. Therefore, obviously, the gauge field is in general non-abelian. The remarkable thing about \mathbf{A} is that it is easily programmable by an appropriate choice of magnetic field gradients. Choosing for instance only a field gradient of one magnetic field component leaves us with only one component of the angular momentum and we thus get an abelian gauge potential. Choosing arbitrary linear combinations of angular momentum operators is only restricted by the properties of the real physical magnetic field employed, in particular $\text{div} \mathbf{B} = 0$, as we shall see below.

Before working out a few specific examples, three more remarks:

1. We chose the same trap frequency ω in all directions, which is certainly somewhat unusual for an

optical dipole trap. After canonical transformation, this translates into the same mass for all three directions. Had we different trap frequencies in different directions, we would get effectively different masses in different directions, i.e. a (diagonal) effective mass tensor, similar to the situation in a semiconductor. This may or may not be useful, depending on what one wants to simulate.

2. Similarly, if we kept the quadratic term in the expansion of \mathbf{B} , we would get additional quadratic terms (which would also depend on the internal state of the atom) contributing to the trapping potential, such that, again, after the canonical transformation we would end up with different masses in different directions.
3. What was derived here for a single atom should translate immediately to a BEC, if the interactions between atoms are negligible. If they are not, any interaction potential $V(\mathbf{x}_i - \mathbf{x}_j)$ will translate into a momentum dependent interaction after the canonical transformation.

Let us now look at some concrete examples of non-Abelian gauge potentials, inspired by the list in [8]. I will assume that we have an atom with $J = 1/2$, so that the J_i are given by Pauli-matrices, $J_i = (\hbar/2)\sigma_i$.

Rashba coupling. This is a coupling $\alpha(p_y \sigma_z - p_z \sigma_y)$, with some constant α . It can easily be achieved by choosing $\partial_x B_i = 0$, for $i = x, y, z$, $\partial_y B_y = 0 = \partial_z B_z$, and $\partial_y B_z = B' = \partial_z B_y$. No magnetic mono-pole is required, $\text{div} \mathbf{B} = 0$, but the field has a finite curl in x -direction, $(\nabla \times \mathbf{B})_x = 2B'$. That curl is needed at $\mathbf{x} = \mathbf{0}$, where we did the expansion of the magnetic field. But since we insisted on a linearly growing field over the lengthscale of the motion in the trap, we request basically circular magnetic field lines around the x -axis, with magnetic field strength growing linearly with distance from the x -axis. That is, of course, quite different from what a current carrying wire along the x -axis would do (apart from the fact that that wire would have to go straight through $\mathbf{x} = \mathbf{0}$, where we would like to trap the atom). A possible way of creating the required magnetic field might be through an electric field that increases linearly in time by using segmented cylindrically arranged electrodes. Choosing the right voltage profile for all the electrodes one can create a radially symmetric electric field oriented in x -direction that increases proportionally in radial direction, and generates the desired \mathbf{B} -field according to Maxwell's equation $\nabla \times \mathbf{H} = \dot{\mathbf{D}} + \mathbf{j}$.

The inverse tensor of inertia is here simply $I^{-1} = \text{diag}(0, B'^2, B'^2)$ and just leads to a constant $\phi = B'^2 \mathbf{1}$, i.e. an identity matrix in spin Hilbert-space.

Linear Dresselhaus coupling. Here we want $A_y = \alpha\sigma_y$, $A_z = -\alpha\sigma_z$. Choose again $\partial_x B_i = 0 \forall i$, but then $\partial_y B_y = B' = -\partial_z B_z$, and all other derivatives equal zero. Again, this is compatible with $\text{div}\mathbf{B} = 0$, and we basically get a field that is point symmetric, growing linearly in radial direction, but pointing towards the center on the z -axis and outward on the y -axis, like from a quadrupole magnet.

Inverse tensor of inertia and the resulting potential ϕ are identical to the Rashba case.

Graphene sheet in vicinity of Dirac point. This case is more problematic: we want $A_y = \alpha\sigma_y$, $A_z = \alpha\sigma_z$, which leads to $\partial_y B_y = B' = \partial_z B_z$. But $\text{div}\mathbf{B} = 0$ then requires $\partial_x B_x = -2B'$, and thus adds an extra coupling term $-2p_x\sigma_x$ to the desired $p_y\sigma_y + p_z\sigma_z$.

Zitterbewegung. *Zitterbewegung* (ZB) is an interference effect first predicted by Schrödinger for relativistic spin-1/2 particles that leads to a jittering motion on the length scale of the Compton wavelength of the particle, i.e. $\hbar/mc \simeq 10^{-12}\text{m}$ for an electron [7]. This short length scale has so far prevented direct experimental observation of ZB for relativistic electrons. However, the effect should exist for any spinor system with linear dispersion relation. Consequently, ZB has been studied theoretically in several systems, including mesoscopic wires [9], graphene [10], ion traps [11], and optical lattices [8]. Rashba couplings in quantum dots with rotationally invariant potentials in 2D was studied in [12]. Very recently, ZB was observed experimentally with a single trapped ion [13]. ZB has mostly been studied for a free particle. The ZB then dies out after a short time, when the two wave-packages corresponding to spin-up and spin-down have separated enough to prevent further interference. It is interesting to consider how the additional harmonic confinement potential in (5) modifies the ZB. One might expect that the confinement will increase the time interval in which the ZB can be observed.

We now study ZB for the harmonic confinement (5) in the Rashba case. We show that ZB exists even if the harmonic oscillator is initially unexcited, and that it can persist for arbitrarily long times. Note that the third direction, x in the above notation, is not affected by the gauge field and just separates. It is convenient then, to rewrite (5) in terms of annihilation (creation) operators $a(a^\dagger)$ and $b(b^\dagger)$ for the y and z components, respectively. We are thus lead to

$$H = \hbar\omega (a^\dagger a + b^\dagger b + ib_1 (-(a - a^\dagger)\sigma_z + (b - b^\dagger)\sigma_y) + \mathbf{b}_0 \cdot \boldsymbol{\sigma}), \quad (13)$$

where the dimensionless parameters are $b_1 = \frac{g_J \mu_B B'}{2\sqrt{\hbar m \omega^3}}$ and $\mathbf{b}_0 = \frac{\mu_B g_J \mathbf{B}(0)}{2\hbar\omega}$, and we have suppressed an irrelevant constant.

It is straightforward to express H in basis states $|nms\rangle$, where $n, m \in \{0, 1, 2, \dots\}$ are the occupation numbers for oscillators a and b , and $s \in \{\pm 1\}$ label eigenstates of σ_z corresponding to these eigenvalues, and to diagonalize the Hamiltonian numerically. This basis turns out to be highly suitable — taking into account only up to 5 excitations per oscillator (i.e. a 72 dimensional basis) allows one to find the lowest 26 eigenstates already with 4 significant digits for $b_1 = 0.1$ (compared to the case with 10 excitations per oscillator, or 242 basis states, which we used in the numerical simulations). With the obtained propagator we can study the time evolution of the averages of the observables $\langle y(t) \rangle$, $\langle p_y(t) \rangle$ etc.

Figure 1 shows $\langle y(t) \rangle$ for $\mathbf{b}_0 = \mathbf{0}$, different values of b_1 , and the two initial states $|\psi(0)\rangle = |00+\rangle$ and $|00-\rangle$. Both $\langle z(t) \rangle$ and $\langle p_z(t) \rangle$ remain always zero in these cases, whereas $\langle y(t) \rangle$ shows oscillations. They are always with opposite sign for these two different initial states. For small values of b_1 ($b_1 = 0.1$) the oscillations appear periodic, whereas with increasing b_1 , additional harmonics appear that make the signal look more and more erratic. By changing the initial state of the spin, the direction of the oscillation can be chosen. E.g. for $|\psi(0)\rangle = (|00+\rangle + i|00-\rangle)/\sqrt{2}$, we obtain $\langle y(t) \rangle = 0 = \langle p_y(t) \rangle$, whereas the z -component now shows the signal we had for $\langle y(t) \rangle$. The state $|\psi(0)\rangle = (\cos(\pi/8)|00+\rangle + i\sin(\pi/8)|00-\rangle)$ leads to oscillations with $\langle y(t) \rangle = -\langle z(t) \rangle$. It appears thus that the ZB is always one-dimensional as long as the initial state is chosen in the subspace $\{|00+\rangle, |00-\rangle\}$. The superposition $|\psi(0)\rangle = (|00+\rangle + |00-\rangle)/\sqrt{2}$ switches the ZB off in both components. Note that one-dimensional ZB was also predicted for a 1D harmonic confinement and a specific initial spin state, with the ZB perpendicular to the free 1D motion [9].

The results for small b_1 can be easily understood analytically, by going to the Heisenberg picture and expanding the time dependent operators to lowest order in b_1 . We find, correct to order $\mathcal{O}(b_1)$, at $\mathbf{b}_0 = \mathbf{0}$

$$\langle y(t) \rangle \simeq \langle y(0) \rangle \cos \omega t + \langle p_y(0) \rangle \sin \omega t + \sqrt{2}b_1 \langle \sigma_z(0) \rangle \sin \omega t \quad (14)$$

$$\langle z(t) \rangle \simeq \langle z(0) \rangle \cos \omega t + \langle p_z(0) \rangle \sin \omega t - \sqrt{2}b_1 \langle \sigma_y(0) \rangle \sin \omega t \quad (15)$$

$$\langle p_y(t) \rangle \simeq \langle p_y(0) \rangle \cos \omega t - \langle y(0) \rangle \sin \omega t + \sqrt{2}b_1 \langle \sigma_z(0) \rangle (\cos \omega t - 1) \quad (16)$$

$$\langle p_z(t) \rangle \simeq \langle p_z(0) \rangle \cos \omega t - \langle z(0) \rangle \sin \omega t - \sqrt{2}b_1 \langle \sigma_y(0) \rangle (\cos \omega t - 1). \quad (17)$$

All positions and momenta are expressed in terms of the length-scales x_0 and momentum scales p_0 of the harmonic oscillator, respectively. The corrections to Eqs.(14-17) are of order $\mathcal{O}(B_1^2)$. We recognize in the terms independent of b_1 the unperturbed motion of the 2D harmonic

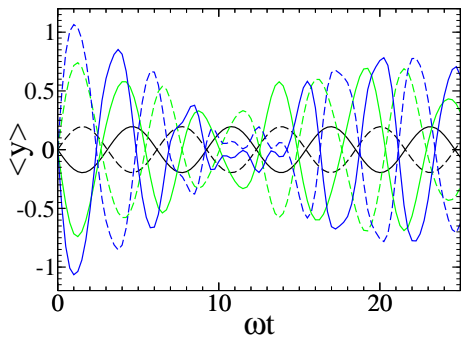


FIG. 1: (Color online) *Zitterbewegung* in $\langle y(t) \rangle$ (in units of harmonic oscillator length x_0) for initial states $|00+\rangle$ (full lines) and $|00-\rangle$ (dashed lines); $\mathbf{b}_0 = \mathbf{0}$, and b_1 takes the values $b_1 = 0.1, 0.5$ and 1 for black lines, green (light grey) lines, and blue lines (dark grey), respectively.

oscillator. This motion can be switched off by choosing average initial positions and momenta equal zero, as is the case for the initial states discussed above with the two harmonic oscillators initially in their ground state. All motion is then entirely due to the ZB and indeed 1D, in a direction given by the vector $(\langle \sigma_z(0) \rangle, \langle \sigma_y(0) \rangle)$. Interestingly, at $|b_1| \ll 1$ the ZB is itself harmonic with an amplitude controlled by b_1 . The fact that the length and momenta scales of the ZB are set by the harmonic confinement should allow for a much simpler experimental verification than for Dirac electrons. Moreover, the harmonic confinement potential keeps the wavepackages corresponding to the two different spin components together, preventing the decay of the ZB, which should facilitate its experimental study. A damping of the ZB can arise at higher values of b_1 and initial coherent states of the harmonic oscillators, which will in general be smeared out due to the anharmonicity mediated by the coupling to the spin (see Figs.2 and 3). At $b = 1$ the dynamics looks random and diffusive in the yz -plane, but the trajectory of average values $(\langle y(t) \rangle, \langle z(t) \rangle)$ is of course entirely deterministic and reproducible.

The increasingly erratic behavior of the ZB with increasing b_1 can be understood by looking at the spectrum of H , plotted in Fig.4. The oscillator states at $b_1 = 0$ containing n energy quanta which are $2(n+1)$ -fold degenerate (states $|n0+\rangle, |n-1+\rangle, \dots, |n0-\rangle$, and the same set once more but with spin down). They split with increasing b_1 and lead to several avoided crossings. The resulting incommensurate frequencies lead to the observed quasi-periodic, apparently random behavior.

In summary, we have shown how a single trapped atom with hyperfine structure trapped in a magnetic field with suitably tailored field gradients can be used to simulate the effect of non-abelian gauge potentials. We have demonstrated how different effective spin-orbit couplings (such as Rashba or linear Dresselhaus couplings) can be easily obtained, and we have proposed a new way of ob-

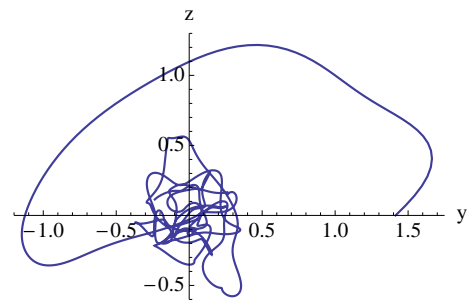


FIG. 2: (Color online) Trajectory of 2D *Zitterbewegung* in $(\langle y(t) \rangle, \langle z(t) \rangle)$ (in units of harmonic oscillator length x_0) for an initial state $|\alpha\beta+\rangle$, where $|\alpha\rangle$ and $|\beta\rangle$ are coherent states with $\alpha = 1$ and $\beta = i$ at $\mathbf{b}_0 = \mathbf{0}$ and $b_1 = 1$. The trajectory is shown for $0 \leq \omega t \leq 50$. The initial state is localized at $\langle y(0) \rangle = \sqrt{2} = \langle p_z(0) \rangle$, $\langle z(0) \rangle = 0 = \langle p_y(0) \rangle$ and would lead for $b_1 = 0$ to circular motion in the yz -plane.

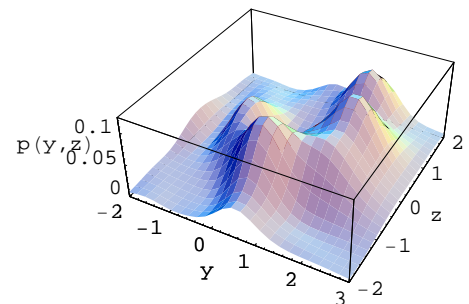


FIG. 3: (Color online) Probability distribution $p(y, z)$ of finding the atom localized at position y, z (in units of x_0) at $\omega t = 10$, for $b_1 = 1.0, \mathbf{b} = \mathbf{0}$. The initial coherent state (same state as in Fig.2) gets smeared out due to the anharmonicity created by the Rashba coupling.

serving *Zitterbewegung* of a harmonically trapped particle. An immediate consequence of the fact that (5) was obtained by a canonical transformation that exchanges position and momentum, is that the ZB in $y(t)$ will, of course, show up in $p_y(t)$ in the original system. The simplicity and flexibility of the proposed setup may also allow the study of other spin-orbit couplings, as well as of applications such as robust quantum gates based on topological phases [14].

Acknowledgements: I would like to thank the JQI (University of Maryland and NIST Gaithersburg) for hospitality during my stay during which this work was started, and Victor Galitski, Trey Porto, Bill Phillips, Ian Spielman, and Jay Vaishnav for discussions.

[1] M. Greiner, O. Mandel, T. Esslinger, T. W. Hänsch, and I. Bloch, *Nature* **415**, 39 (2002).

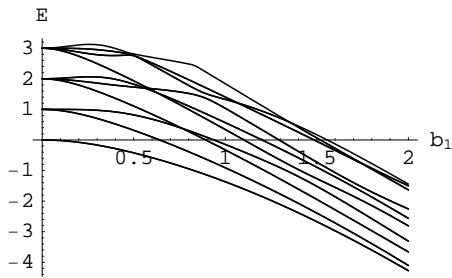


FIG. 4: Lowest 20 energies in the Spectrum of H in units of $\hbar\omega$ as function of b_1 at $\mathbf{b}_0 = \mathbf{0}$. The spectrum is symmetric under $b_1 \rightarrow -b_1$, and each energy level shown is still doubly degenerate.

[2] J. Billy, V. Josse, Z. Zuo, A. Bernard, B. Hambrecht, P. Lugan, D. Clement, L. Sanchez-Palencia, P. Bouyer, and A. Aspect, *Nature* **453**, 891 (2008), ISSN 0028-0836, URL <http://dx.doi.org/10.1038/nature07000>.
 [3] G. Roati, C. D'Errico, L. Fallani, M. Fattori, C. Fort, M. Zaccanti, G. Modugno, M. Modugno, and M. Inguscio, *Nature* **453**, 895 (2008), ISSN 0028-0836, URL <http://dx.doi.org/10.1038/nature07071>.

[4] U. Leonhardt and P. Piwnicki, *Physical Review Letters* **84**, 822 (2000), ISSN 0031-9007, URL http://prl.aps.org/abstract/PRL/v84/i5/p822_1.
 [5] Y. Lin, R. L. Compton, K. Jimenez-Garcia, J. V. Porto, and I. B. Spielman, *Nature* **462**, 628 (2009), ISSN 0028-0836, URL <http://dx.doi.org/10.1038/nature08609>.
 [6] V. Pietilä and M. Möttönen, *Phys. Rev. Lett.* **103**, 030401 (2009).
 [7] E. Schrödinger, *Die Naturwissenschaften* **24**, 418 (1930).
 [8] J. Y. Vaishnav and C. W. Clark, *Physical Review Letters* **100**, 153002 (pages 4) (2008), URL <http://link.aps.org/abstract/PRL/v100/e153002>.
 [9] J. Schliemann, D. Loss, and R. M. Westervelt, *Phys. Rev. Lett.* **94**, 206801 (2005).
 [10] J. Cserti and G. Dávid, *Phys. Rev. B* **74**, 172305 (2006).
 [11] L. Lamata, J. León, T. Schätz, and E. Solano, *Phys. Rev. Lett.* **98**, 253005 (2007).
 [12] E. Tsitsishvili, G. S. Lozano, and A. O. Gogolin, *Physical Review B (Condensed Matter and Materials Physics)* **70**, 115316 (pages 11) (2004), URL <http://link.aps.org/abstract/PRB/v70/e115316>.
 [13] R. Gerritsma, G. Kirchmair, F. Zähringer, E. Solano, R. Blatt, and C. F. Roos, 0909.0674 (2009), URL <http://arxiv.org/abs/0909.0674>.
 [14] A. Kitaev, *quant-ph/9511026*.